J Radioanal Nucl Chem (2012) 292:501–512
DOI 10.1007/s10967-011-1436-9

Binary biosorption of uranium(VI) and nickel(II) from aqueous solution by Ca-pretreated *Cystoseira indica* in a fixed-bed column

Ali Reza Keshtkar · Fatemeh Kafshgari · Mohammad Ali Mousavian

Received: 4 September 2011 / Published online: 20 September 2011

Abstract Simultaneous biosorption of uranium(VI) and nickel(II) ions onto Ca-pretreated *Cystoseira indica* biomass was studied and compared with single uranium or nickel biosorption in a fixed-bed column. Results of single biosorption showed the breakthrough and exhaustion time increase with the increase of the flow rate and inlet metal concentration for both metal ions. Also, it was observed that there was an optimum flow rate of 1.4 mL min^{-1} (surface loading of 0.792 cm min^{-1}) for both metal ions in the column. Results from both single and binary systems showed the adsorption capacity of *C. indica* for both metal ions increases with the increasing inlet concentration of each component and *C. indica* had a stronger affinity for uranium than nickel ions. The binary system results showed that the presence of the second component affected the adsorption of the first one by *C. indica* so the antagonistic action was observed. Also, the inhibitory effect of uranium ions on the nickel adsorption was greater than nickel ions on the uranium adsorption. The uranium and nickel breakthrough curves under different conditions were described by the Thomas, Yoon-Nelson and Yan models. Among these models, the Yan model appeared to describe the experimental results better.

Keywords Biosorption · Fixed-bed bioreactors · Dynamic modeling · Separation · Uranium(VI) · Nickel(II)

A. R. Keshtkar (✉)
Nuclear Fuel Cycle School, Nuclear Science and Technology Research Institute, P.O. Box 11365-8486, Tehran, Iran
e-mail: akeshtkar@aeoi.org.ir

F. Kafshgari · M. A. Mousavian
Department of Chemical Engineering, Faculty of Engineering, University of Tehran, P.O. Box 11155-4563, Tehran, Iran

List of symbols

Variables

a	Yan empirical parameter
C_t	Effluent uranium concentration at time of t (mg L^{-1})
C_0	Influent metal concentration (mg L^{-1})
K_a	Rate constant (L mg^{-1} min^{-1})
k_{Th}	Thomas rate constant (L min^{-1} g^{-1})
K_{YN}	Yoon-Nelson rate constant (L min^{-1} g^{-1})
M	Dry weight of biosorbent (g)
m_{ad}	The quantity of metal retained in the column (g)
m_d	Metal mass desorbed (g)
m_{total}	Total amount metal sent to column (g)
Q	Flow rate (L min^{-1})
q_0	Maximum uptake capacity (mg g^{-1})
t	Service time (h)
t_b	Breakthrough time (h)
t_e	Bed exhaustion time (h)
$t_{0.5}$	Time at which the effluent concentration is half the influent (h)
V_e	Effluent volume (L)
v	Linear velocity (cm min^{-1})

Greek letters

τ_i	The time required for 50% of i adsorbate breakthrough (h)

Introduction

An expansion of several industrial sectors leads to an increasing demand for the usages of heavy metals. Despite an advance in pollution control techniques, heavy metals still could find their ways to the environment particularly through wastewater discharge or leachate of solid waste.

The abatement of wastewater containing heavy metals can be achieved via several techniques such as precipitation, evaporation, etc. However, these common treatment processes have been shown to be quite expensive and ineffective for low strength wastewaters [1]. Among these, the adsorption technique is considered to be very important because of its cost effective treatment, easy operation, narrow space for building the plant, no chemical reagents needed and no sludge produced [2]. The search for an uncostly and easily available adsorbent has led to the investigation of materials of agricultural and biological origin, along with industrial byproducts, as adsorbents [3]. Biosorption, the process of passive cation binding by dead or living biomass, represents a potentially cost effective way of removing toxic metals from industrial wastewaters [4]. Biosorption is the ability of certain types of microbial biomass to accumulate heavy metals from aqueous solutions [5]. The potential of biosorption depends on the metal uptake capacities, selectivity, and ease of metal recovery and economics [6]. Biosorption has been successfully used in the treatment of metal contaminated water using low cost materials, such as, marine algae, bacteria, fungi, industrial wastes and several other materials [7]. Of the many types of biosorbents recently investigated for their ability to sequester heavy metals, the brown algal biomass has proven to be highly effective as well as reliable and predictable in the removal of, for example, Pb^{2+}, Cu^{2+}, Cd^{2+}, $UO_2{}^{2+}$, Ni^{2+} and Zn^{2+} from aqueous solutions [8]. Most separation and purification processes that employ sorption technology use continuous flow columns. In biosorption applications, a fixed bed column is an effective process for continuous wastewater treatment, as it makes the best use of the concentration difference known to be a driving force for heavy metal biosorption and allows more efficient utilization of biosorbent capacity and results in a better quality of the effluent [9].

A number of fixed-bed column investigations have been conducted in single systems for uranium [10–14] and nickel [5, 15–22] removal using various adsorbents, adsorbent bed depths, liquid flow rates, inlet metal ion concentrations and size of adsorbents. Results of these studies have generally indicated that operational conditions can influence the removal efficiencies of column, the adsorption capacity of adsorbent and the position and shape of breakthrough curves. However, according to the author's survey, there is no research on the simultaneous bioremoval of U(VI) and Ni(II) ions using biomaterials in fixed-bed columns to date. Among brown algal biomasses in this paper, the *Cystoseria indica* was chosen as biosorbent because it is not only very abundant in coastal area of The Persian Gulf, Iran but also cheap. In our previous researches single biosorption for U(VI) and Ni(II) from aqueous solution by *C. indica* in batch mode was studied and it was observed that the biomass of *C. indica* could be as an adsorbent to bind both metal ions [23–25]. The aim of this study was to develop a new and cheap technology for the removal of heavy metals pollutions from wastewater and other aqueous system. Uranium and nickel were selected as representative heavy metals in this study because they are widely used in various industries and often released into the environment from mining and milling facilities. The objective of this work was to investigate the simultaneous biosorption of U(VI) and Ni(II) ions onto Ca-pretreated *C. indica* biomass and to compare the binary biosorption results with single biosorption results in a fixed-bed column. Also the effect of important parameters, such as the flow rate, the inlet metal ion concentration and the effect of coexistence ions on the effluent metal ion concentration were examined and compared with predictions of the Thomas, Yoon-Nelson and Yan models.

Materials and methods

Preparation of biosorbent

The brown algae, *C. indica* obtained from The Persian Gulf on the coast of Qeshm, Iran was extensively washed with distilled water and sun-dried on the beach and in an oven at 50 °C overnight. The dried biomass was ground in a laboratory blender and sorted using the standard test sieves. The batch of biomass with particle size 1.0–1.25 mm was selected for subsequent Ca-pretreatment. Ca-pretreatment of the biomass was carried out as follows: a sample of 10 g of biomass was treated with 0.1 M $CaCl_2$ solution (1000 mL) for 12 h under slow stirring.

Biosorption experiments

All of the experiments were performed in a fixed-bed column at room temperature (25 ± 2 °C). The column was a simple glass tube with a bore of 1.5 cm and a length of 10 cm. Two plastic sieves both with pore size of 0.5 mm were installed at the top and bottom of this column. The experiments were conducted by pumping a metal solution in up flow mode through the fixed-bed column with a peristaltic pump (Watson Marlow Pumps, Model 205U). A weight of 1 g of the dry biosorbent (equal to 4 cm bed height) was packed within the column. The porosity (bed void volume to bed volume ratio) of the wet biosorption bed was 41% in the fixed-bed column. Liquid samples of the column effluent were collected at predefined time intervals and were analyzed for residual heavy metal (UO_2^{+2} and Ni^{2+}) concentration by an inductively coupled plasma spectroscopy (ICP, Varian, Model Liberty 150 AX Turbo). The ICP analyses were conducted at wavelength of

385.95 and 221.84 nm, respectively. The synthetic solutions were all prepared by the use of deionized water and analytical grade salts of UO_2 $(NO_3)_2{\cdot}6H_2O$ and Ni $(NO_3)_2{\cdot}6H_2O$ (Merck supplied). The pH of influent solutions was measured with a pH meter (Metrohm, Model 780) and adjusted by using 0.1 M HCl and/or 0.1 M NaOH solution. The optimum pH values for single biosorption of U(VI) and Ni(II) onto *C. indica* biomass obtained were 4 and 6, respectively in our previous studies [23, 26]. Therefore, in this study the pH of influent solutions was adjusted to 4 and 6 for investigation of flow rate effect on single biosorption of U(VI) and Ni(II), respectively and to 4 for investigation of inlet metal ion concentration effect on single and binary biosorption of both metal ions. The metal ions solution containing uranium and/or nickel in different concentrations from 30 to 90 mg L^{-1} were applied to the column. Operation of the column was stopped when the effluent metal concentration reached a constant value (equal to the influent metal concentration).

Modeling and analysis of column data

Design and optimization of fixed-bed columns are difficult to carry out a priori without a quantitative modeling approach. From the perspective of process modeling, the dynamic behavior of a fixed bed column is described in terms of the effluent concentration—time profile, i.e. the breakthrough curve. The time for breakthrough appearance and the shape of the breakthrough curve are very important characteristics for determining the operation and the dynamic response of a biosorption column. The general position of the breakthrough curve along the time (or effluent volume) axis depends on the capacity of the column with respect to the bed height, flow rate and feed concentration. The breakthrough curve would be a step function for favorable separations, i.e. there would be an instantaneous jump in the effluent concentration from zero to the feed concentration at the moment the column capacity is reached [26–29]. The breakthrough time (t_b) is the time at which metal concentration in the effluent reached 5% of the influent value and the bed exhaustion time (t_e) is the time at which metal concentration in the effluent exceeded 95% of the influent value. Also, the effluent volume (V_e) that is the volume of metal solution passed into the column (mL) can be calculated as follows [21, 26]:

$$V_e = Q \times t \tag{1}$$

where t is time (min) and Q is the volumetric flow rate (mL min^{-1}). The breakthrough curves indicate the loading behavior of algal biomass for U(VI) and/or Ni(II) (i component) to be removed from solution in a fixed-bed and is usually expressed in terms of normalized concentration, defined as the measured effluent concentration of metal ions, C_i (mg L^{-1}) divided by the inlet concentration of metal ions, $C_{0,i}$ (mg L^{-1}) as a function of time (t) or throughput volume for a given bed height. The area above the plot of normalized concentration of i component versus time obtained by numerical integration, can be used to find the total adsorbed quantity of i component, $m_{ad,i}$ (mg) for a given feed concentration and flow rate as follows:

$$m_{ad,i} = \frac{Q \times C_{0,i}}{1000} \int_{t=0}^{t=t_e} \left(1 - \frac{C_i}{C_{0,i}}\right) dt \tag{2}$$

Dividing the metal mass adsorbed ($m_{ad,i}$) by the mass of alga in the bed, M (g) leads to the equilibrium uptake capacity of the biosorbent (q_i) [21, 30, 31].

$$q_i = \frac{m_{ad,i}}{M} \tag{3}$$

Total amount of i component sent to column, $m_{total,i}$ (mg) can be found from Eq. 4

$$m_{total,i} = \frac{C_{0,i} \times Q \times t_e}{1000} \tag{4}$$

Total removal percent of i component can be calculated from Eq. 5

$$Ad(\%) = \frac{m_{ad,i}}{m_{total,i}} \times 100 \tag{5}$$

For binary mixture, total removal percent of U(VI) and Ni(II) can be also found from the ratio of total adsorbed quantity of both U(VI) and Ni(II) ions to the total amounts of U(VI) and Ni(II) sent to column, as follows:

$$Ad_{total}(\%) = \frac{\sum m_{ad,i}}{\sum m_{total,i}} \times 100 \tag{6}$$

Finally, total equilibrium uptake capacity of U(VI) and Ni(II) in the column is defined by Eq. 7 as the total amount of two components sorbed per the mass of alga in the bed.

$$q_{total} = \frac{\sum m_{ad,i}}{M} \tag{7}$$

The mathematical modeling has a key role in the scale up procedure from laboratory experiments through pilot plant to industrial scale [16]. Developing a model to describe accurately the dynamic behavior of adsorption in a fixed bed system under given specific operating conditions is inherently difficult. Because of the concentration of the adsorbate as the feed moves through the bed, the process does not operate at steady state. The fundamental transport equations derived to model the fixed bed with theoretical rigor are differential in nature and usually require complex numerical methods to solve. Various simple mathematical

models have been developed to predict the dynamic behavior of the column. These models are useful for the sizing and optimization of the industrial scale processes [32]. Below, the three simple models are described. To choose them, the conditions of application of each one of them and their use for the study of biosorption in a column have been considered by the majority of researchers.

The Thomas model

One of the most general and widely used models to describe the behavior of the biosorption process in fixed-bed columns is the Thomas model which is derived from the equation of the mass conservation in a flow system [33]. The main limitation of Thomas model is that its derivation is based on the second order kinetics and considers that sorption is not limited by the chemical reaction but controlled by the mass transfer at the interface. This discrepancy can lead to errors when this method is used to model biosorption processes in specific conditions [26]. This model can be described by the following expression:

$$\frac{C_{\mathrm{i}}}{C_{0,\mathrm{i}}} = \frac{1}{1 + \exp\left(\frac{M \times q_{0,\mathrm{i}} \times k_{\mathrm{Th,i}}}{Q} - \frac{C_{0,i} \times k_{\mathrm{Th,i}} \times t}{1000}\right)} \tag{8}$$

where $k_{\mathrm{Th,i}}$ is the Thomas rate constant (L min^{-1} g^{-1}) of i component and $q_{0,\mathrm{i}}$ is the maximum uptake capacity (mg g^{-1}) of i component. The model parameters $k_{\mathrm{Th,i}}$ and $q_{0,\mathrm{i}}$ can be estimated by non-linear fitting of Eq. 8 to the experimental data of breakthrough curves.

The Yoon and Nelson model

Yoon and Nelson [34] have developed a relatively simple model addressing the adsorption and breakthrough of adsorbate vapors or gases with respect to activated charcoal. This model assumes that the rate of decrease in the probability of adsorption for each adsorbate molecule is proportional to the probability of sorbate sorption and the probability of sorbate breakthrough on sorbent [35].The Yoon and Nelson equation to each component in a single and in a binary system is expressed as:

$$\frac{C_{\mathrm{i}}}{C_{0,\mathrm{i}}} = \frac{\exp\left(K_{\mathrm{YN,i}} \times \frac{t}{60} - K_{\mathrm{YN,i}} \times \tau_{\mathrm{i}}\right)}{1 + \exp\left(K_{\mathrm{YN,i}} \times \frac{t}{60} - K_{\mathrm{YN,i}} \times \tau_{\mathrm{i}}\right)} \tag{9}$$

where $k_{\mathrm{YN,i}}$ is the Yoon and Nelson rate constant of i component (h^{-1}), τ_{i} the time required for 50% of i adsorbate breakthrough (h), and t is the sampling time (min). The calculation of theoretical breakthrough curves for i component requires the determination of the parameters $k_{\mathrm{YN,i}}$ and τ_{i}.

The Yan model

The Yan model is based on statistical analysis of experimental data and some simplifications [36]. This model can be represented by:

$$\frac{C_{\mathrm{i}}}{C_{0,\mathrm{i}}} = 1 - \frac{1}{1 + \left(\left(\frac{0.001 \times C_{0,\mathrm{i}} \times Q}{q_{0,\mathrm{i}} \times M}\right) \times t\right)^{a_{\mathrm{i}}}} \tag{10}$$

where a_{i} and $q_{0,\mathrm{i}}$ are the model parameters. Yan model has a relative importance because it normally describes the complete breakthrough curves with great accuracy. However, it is difficult to relate the empirical parameter "a" with the experimental conditions, so the scale up of the system is impossible [30].

Results and discussion

The effect of flow rate

The feed flow rate is an important variable affecting biosorption process of heavy metals in fixed-bed columns because the transfer process, especially at a low metal concentration, is usually under the mass-transfer-controlled mode. Therefore, in order to investigate the effect of feed flow rate on the single-component biosorption of U(VI) and Ni(II) ions by *C. indica*, the inlet metal concentration in the feed was held constant at 30 mg L^{-1} while the flow rate was changed from 0.7 to 2.1 mL min^{-1}. The empty bed contact time (EBCT) of metal ions through the column changed from 10 to 3.5 min. The plots of the ratio of effluent to influent metal ion concentrations versus time at different feed flow rate for the adsorption of U(VI) and Ni(II) are presented in Fig. 1a and b, respectively. Also the results of the breakthrough curves analysis are given in Table 1. As expected, the breakthrough curves shifted towards a lower time scale and became steeper with increasing flow rate for both metal ions. Also, the breakthrough time and exhaustion time decreased from 55.15 to 11.72 h and from 255.14 to 110.4 h, respectively for U(VI) ions and from 12 to 1.4 h and 72 to 45 h, respectively for Ni(II) ions as the flow rate increased from 0.7 to 2.1 mL min^{-1}. This indicates a shorter column active life at a higher feed flow rate. This behavior may be due to insufficient residence time of the solute in the column, which causes the metal ion solution to leave the column before equilibrium occurs. Indeed, according to the batch experiments, the time required to reach an equilibrium state between *C. indica* and U(VI) and Ni(II) ion solutions is approximately 2 h for both ions [23, 24]. As can be seen from Table 1, the uranium and nickel adsorption columns containing 1 g (dry weight) of the biomass could purify

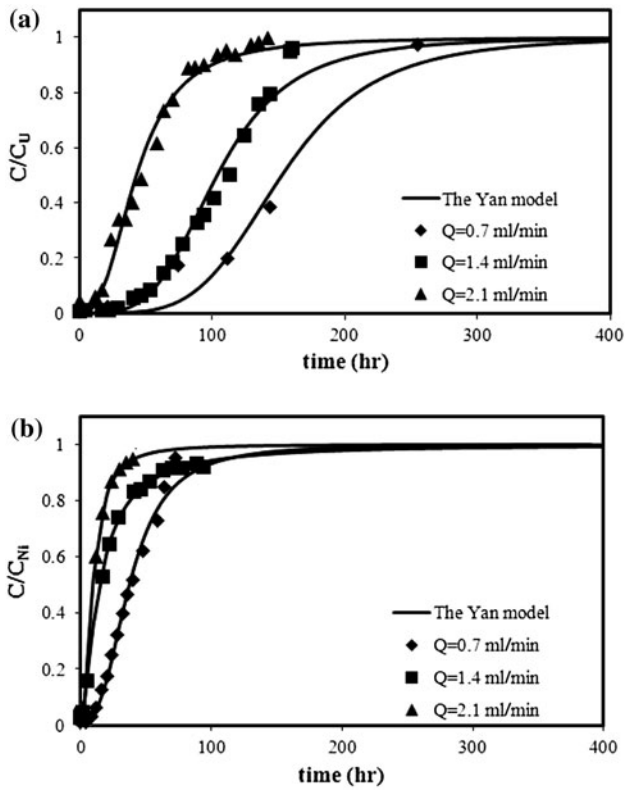

Fig. 1 The experimental and predicted breakthrough curves of single U(VI) (**a**) and single Ni(II) (**b**) obtained at different flow rates

2.32 and 0.5 L of 30 mg L^{-1} metal solution at 0.7 mL min^{-1} feed flow rate before breakthrough, respectively. The highly treated solution volume of uranium with respect to nickel showed that this alga had the greatest sorption capacity for U(VI).

On the other hand, the results showed that in the range of low flow rates (high residence times), the overall rate of metal ions removal in the fixed-bed column was controlled by external mass transfer limitations. In this range, the metal uptake capacity was strongly influenced by increasing flow rate from 0.7 to 1.4 mL min^{-1}, so that, its value for uranium and nickel increased from 175.7 to 238.6 mg g^{-1} and from 44.4 to 52.0 mg g^{-1}, respectively.

Generally, when the biosorption process is under external mass-transfer-controlled mode, a higher flow rate leads to a higher metal biosorption rate since the liquid film resistance to mass transfer of metal ions from the bulk liquid to the biosorption surface is reduced with an increase in the liquid flow rate. The external mass-transfer-controlled mode in fixed-bed columns was reported by other investigators [17, 37]. However, above a certain flow rate, the uranium and nickel removal capacity starts to decrease and the overall rate of metal sorption by *C. indica* biomass is controlled by diffusion limitations of the solute into the pores of sorbent. Similar observation was reported by other investigators [1, 3, 38–40].

As can be seen from Table 1 when the flow rate was increased from 1.4 to 2.1 mL min^{-1}, the liquid residence time in the column decreased from 5 to 3.5 min, resulting in less metal ions adsorbed to the biomass, and hence, the uranium and nickel removal capacity was decreased from 238.6 to 165.9 mg g^{-1} and from 52.8 to 46.3 mg g^{-1}, respectively. By comparing the breakthrough curves of U(VI) and Ni(II) ions we observed that the maximum metal removal capacity was obtained at optimum residence time (or liquid flow rate) of 5 min (1.4 mL min^{-1}) at 30 mg L^{-1} influent metal concentration for both U(VI) and Ni(II) ions. Moreover, the removal of U(VI) changed with liquid flow rate at a higher rate than that of Ni(II). Therefore, it was possible to choose an appropriate flow rate in order to separate uranium ions from nickel ions by a *C. indica* fixed-bed column.

The effect of initial concentration of metal ions

One of the parameters that strongly affect the metal removal capacity as well as the general position of the breakthrough curve is the initial metal ion concentration. The breakthrough curves of single uranium(VI) and single nickel(II) obtained by changing initial metal ion concentration from 30 to 90 mg L^{-1} at 0.7 mL min^{-1} flow rate are shown in Fig. 2a and b, respectively. Also, the breakthrough curves analysis of single U(VI) and Ni(II) ions are presented in Table 2. The breakthrough time decreased

Table 1 Column data and parameters obtained at 30 mg L^{-1} inlet metal ion concentration and different flow rates for single biosorption of U(VI) and Ni(II) onto *C. indica* biomass

Metal ion	Q (mL min^{-1})	t_b (h)	t_e (h)	V_{eff} at t_b (L)	V_{eff} at t_e (L)	Uptake capacity (mg g^{-1})	Ad (%)
U(VI)	0.7	55.15	255.14	2.32	10.72	175.71	63
	1.4	40.87	158.75	3.43	13.33	238.64	67
	2.1	11.72	110.40	1.47	13.91	165.93	45
Ni(II)	0.7	12	72	0.504	3.02	44.42	57
	1.4	1.5	70	0.126	5.88	52.05	37
	2.1	1.4	45	0.176	5.67	46.33	30

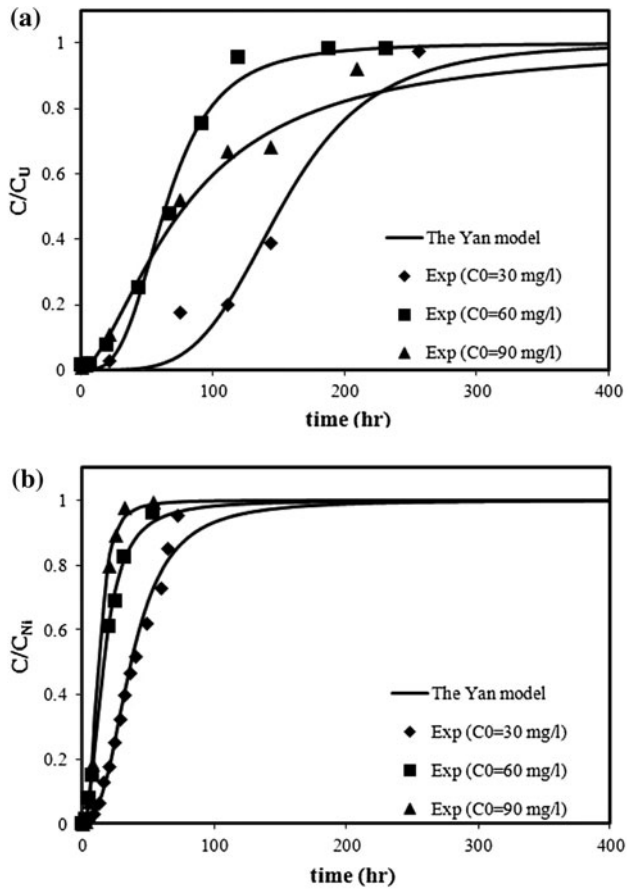

Fig. 2 The experimental and predicted breakthrough curves of single U(VI) (**a**) and single Ni(II) (**b**) obtained at different inlet metal ion concentrations

with an increase in initial concentration for both components. As shown in Fig. 2, breakthrough occurred after 10.66 h and 3.65 h at 90 mg L^{-1} initial concentration of U(VI) and Ni(II) ions, respectively, when the breakpoint time appeared after 55.15 h and 12 h at an initial concentration of U(VI) and Ni(II) ions 30 mg L^{-1}, respectively. Also, as shown in Table 2, the treated volume (or exposure time) was the greatest (10.72 and 3.02 L for U(VI) and Ni(II), respectively) at the lowest inlet concentration since the lower concentration gradient caused a slower transport due to a decreased mass transfer coefficient. As influent concentration increased, the breakthrough curve became steeper and shifted towards the origin for both U(VI) and Ni(II) ions as the binding sites became more quickly saturated in the system at higher initial concentrations. Comparing the case for uranium ions adsorption with that of nickel ions adsorption, it was found that the breakthrough curves for nickel ions were steeper and also breakthrough of nickel occurred faster than uranium. As shown in Table 2, the removal capacity of U(VI) and Ni(II) was increased from 175.7 to 334.3 mg g^{-1} and from 44.4 to 53.4 mg g^{-1} with increasing of initial metal ion concentration from 30 to 90 mg L^{-1}, respectively, while the removal percent of U(VI) and Ni(II) decreased. This result is in agreement with that reported by Han et al.[38], and Aksu's [32] studies. The data in Table 2 also indicated that the dynamic capacity of column for uranium(VI) was significantly greater than that of the nickel(II) due to higher affinity of the sorbent for uranium(VI). In other words, these results showed that the adsorption potential of column for U(VI) and Ni(II) ions on *C. indica* was in the following order: uranium(VI) > nickel(II).

The competitive adsorption of U(VI) and Ni(II) ions

Industrial wastewater usually contains more than one toxic heavy metal ion. Therefore, the effect of competition of multiple metal ions for a limited number of binding sites on biosorption of individual ions was also evaluated. The simultaneous biosorption of U(VI) and Ni(II) ions on *C. indica* in the fixed-bed column was investigated as a function of different combinations of metal ion concentrations in the bimetal solutions. In all simultaneous biosorption experiments, the feed flow rate was held constant at 0.7 mL min^{-1}.

Comparison of individual breakthrough curves of U(VI) and Ni(II) ions obtained in the mixtures containing 30 mg L^{-1} U(VI) ions and 30 mg L^{-1} Ni(II) ions, and containing 90 mg L^{-1} U(VI) ions and 90 mg L^{-1} Ni(II) ions are shown in Fig. 3. For both mixtures the breakthrough curves demonstrated that the adsorption capacity

Table 2 Column data and parameters obtained at 0.7 mL min^{-1} and different inlet metal ion concentrations for single biosorption of U(VI) and Ni(II) onto *C. indica* biomass

Metal ion	C_0 (mg L^{-1})	t_b (h)	t_e (h)	V_{eff} at t_b (L)	V_{eff} at t_e (L)	Uptake capacity (mg g^{-1})	Ad (%)
U(VI)	30	55.15	255.14	2.32	10.72	175.71	63
	60	13.44	216.65	0.56	9.09	194.08	33
	90	10.66	209.1	0.48	8.78	334.34	49
Ni(II)	30	12	72	0.5	3.02	44.42	57
	60	4.01	53.25	0.17	2.23	49.73	40
	90	3.65	29.1	0.15	1.22	53.47	51

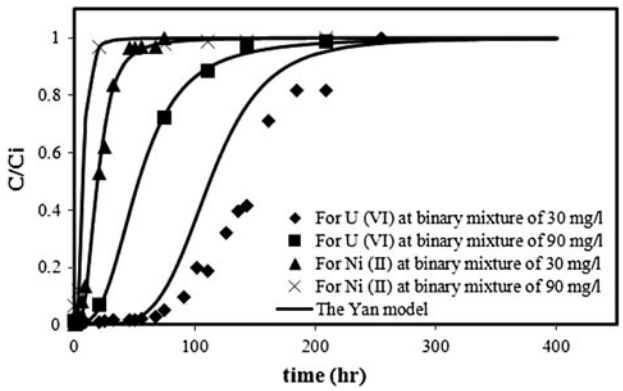

Fig. 3 The experimental and predicted breakthrough curves U(VI) and Ni(II) obtained in the binary mixtures containing 30 mg L^{-1} U(VI) and 30 mg L^{-1} Ni(II) and containing 90 mg L^{-1} U(VI) and 90 mg L^{-1} Ni(II)

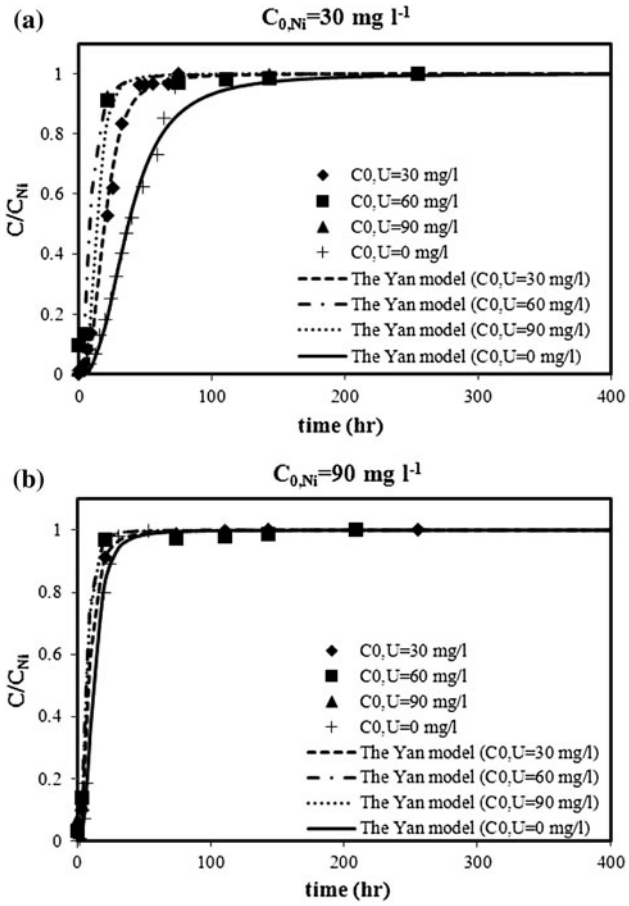

Fig. 4 The experimental and predicted breakthrough curves of Ni(II) at a constant inlet Ni(II) ion concentration of 30 mg L^{-1} (**a**) and 90 mg L^{-1} (**b**) in the absence and in the presence of increasing inlet U(VI) ion concentrations

of the column is different for each component and the data reflect the order of affinity of the biomass very well. A higher adsorption capacity of *C. indica* for U(VI) ions in comparison with Ni(II) ions may be explained on the basis of difference in ionization of U(VI) and Ni(II) ions in aqueous solution and degree of interaction between components and biomass surface [32]. For the mixture containing lower inlet concentrations of both components (30 mg L^{-1} U(VI) and 30 mg L^{-1} Ni(II)), breakthrough curves were more dispersed and breakthrough occurred considerably later than that of other mixture containing higher inlet concentrations of both components. For 30 mg L^{-1} U(VI) and 30 mg L^{-1} Ni(II) containing the mixture, initially, both U(VI) and Ni(II) ions were adsorbed non-selectively due to the competition of both elements for the same binding sites in the biomass so a pollutant-free effluent was produced. With continued treatment, firstly Ni(II) ions began to leave the column followed by U(VI) ions. 176 mg U(VI) and 20.3 mg Ni(II) was adsorbed per gram of *C. indica* biomass in this case(total column capacity was 196.3 mg g^{-1}). An increase in influent concentration of each pollutant appeared to increase the sharpness of the breakthrough curve of each. For 90 mg L^{-1} U(VI) and 90 mg L^{-1} Ni(II) containing mixture, the column capacity of biosorbent was 208.8 mg U(VI) and 47.6 mg Ni(II) per gram of dried biomass (total capacity was equal to 256.4 mg g^{-1}) for this binary system. As shown in Fig. 3 adsorption affinity of the tested metals is U(VI) > Ni(II) which is the same affinity as indicated by the results under non-competitive conditions.

The breakthrough curves of Ni(II) ions obtained at increasing initial U(VI) ion concentrations in the range of 0-90 mg L^{-1} and in constant initial Ni(II) ion concentrations of 30 and 90 mg L^{-1} are shown in Fig. 4a and b, respectively. As shown in Fig. 4, much sharper breakthrough curves but lower adsorption capacities for Ni(II) ions are obtained in higher concentrations of U(VI) ions. The general position of the breakthrough curve along the time axis depends on the capacity of the column with respect to the feed concentration. This is set by the equilibrium [41]. As can be seen in Fig. 4, with a decrease in the inlet concentration of U(VI) ions the breakpoint time and the volume of the feed that can be processed increase and the breakthrough curves shift to the right.

For studies the inhibitory effects Ni(II) ions on the biosorption of U(VI) ions by *C. indica* biomass, the breakthrough curves of U(VI) ions obtained in increasing initial Ni(II) ion concentrations in the range of 0–90 mg L^{-1} and in constant initial U(VI) ion concentration of 30 and 90 mg L^{-1} are shown in Fig. 5a and b, respectively. Similar breakthrough curves were obtained both in the single U(VI) and U(VI)–Ni(II) binary system; the breakthrough curves of uranium became steeper as the concentration of Ni(II) ions in the feed increased. Further, the extent of inhibition in biosorption of uranium was also enhanced with increasing Ni(II) ion concentration. The

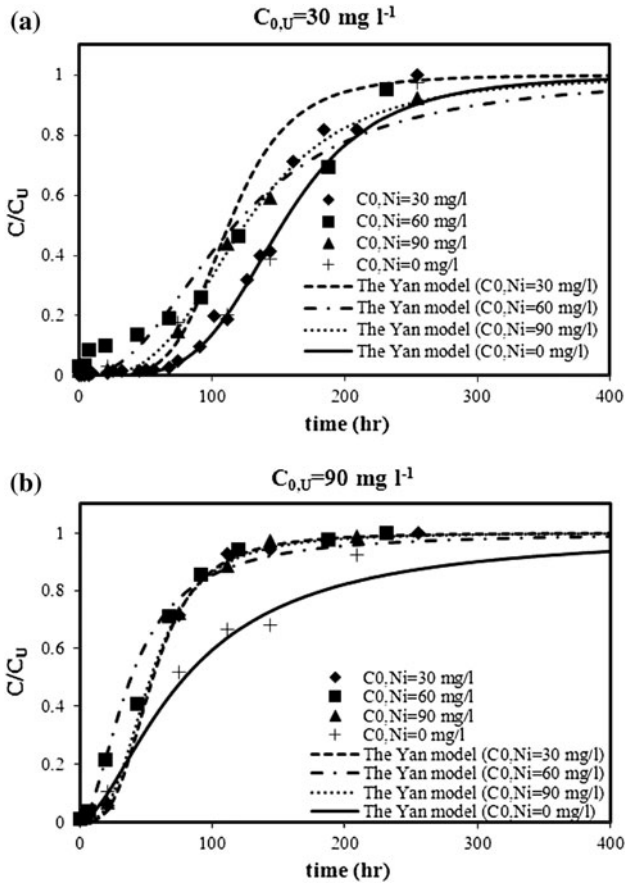

Fig. 5 The experimental and predicted breakthrough curves of U(VI) at a constant inlet U(VI) ion concentration of 30 mg L^{-1} (**a**) and 90 mg L^{-1} (**b**) in the absence and in the presence of increasing inlet Ni(II) ion concentrations

data obtained for U(VI) and Ni(II) biosorption by *C. indica* biomass in binary mixtures prepared in changing concentrations are given in Table 3 in terms of the equilibrium capacity and removal percents of individual U(VI) and Ni(II) ions as well as the total equilibrium capacity and total removal percents of both metal ions. The results in Table 3 indicated that the presence of U(VI) ions has a very lessening effect on the uptake capacity of Ni(II) ions. In 30 mg L^{-1} constant inlet Ni(II) concentration, the reduction of nickel uptake in the presence of 30, 60 and 90 mg L^{-1} U(VI) ion concentrations was 54.3%, 57.5% and 57.8%, respectively. When inlet Ni(II) concentration was held constant at 90 mg L^{-1}, the same inlet U(VI) ion concentrations reduced the nickel uptakes as 4.8%, 6.4% and 10.9%, respectively. Due to these results it can be said that the inhibitory effect of U(VI) ion on the equilibrium nickel uptake is dominant in higher initial U(VI) ion concentrations. The results also indicated that the equilibrium uptake of U(VI) generally decreased with increasing concentrations of Ni(II) ions in the feed. For example, in a 30 mg L^{-1} of constant inlet U(VI) concentration, in the absence of nickel and in the presence of 90 mg L^{-1} nickel in the feed, equilibrium capacity of U(VI) were found as 175.7 and 171.2 mg g^{-1}, respectively. The decrease in the uptake of U(VI) was 2.5% in the presence of 90 mg L^{-1} of Ni(II) ions. When inlet U(VI) concentration was held constant at 90 mg L^{-1}, the effect of 90 mg L^{-1} inlet Ni(II) concentration resulted in a 37.5% reduction in U(VI) uptake. Moreover, the results of Table 3 indicated that a maximum reduction of 57.8% in the adsorption capacity of Ni(II) was observed when U(VI) was present; and a maximum reduction of 37.5% in the adsorption capacity of U(VI) was observed when Ni(II) was present. Therefore, it can be said that the presence of U(VI) ions very greatly affected the uptake of Ni(II) than that of the presence of Ni(II) ions in U(VI) containing solution.

The presence of two or more metals may invoke synergistic or antagonistic responses from an organism. Since the uptake of each metal was strongly influenced and greatly reduced by the presence of other metal, it can be concluded that the combined action of Ni(II) and U(VI) ions is antagonistic. The most logical reason for the antagonistic action is claimed to be the competition for adsorption sites on the cells. The adsorption capacity of U(VI) was also consistently greater than that of Ni(II) for both single-ion adsorption and co-adsorption with the

Table 3 Comparison of the individual and total uptake capacities and individual and total removal percent of U(VI) and Ni(II) ions at 0.7 mL min^{-1} flow rate and different inlet metal ion concentrations for binary biosorption of U(VI) and Ni(II) onto *C. indica* biomass

$C_{0,U}$ (mg L^{-1})	$C_{0,Ni}$ (mg L^{-1})	q_U (mg g^{-1})	q_{Ni} (mg g^{-1})	q_{total} (mg g^{-1})	Ad_U (%)	Ad_{Ni} (%)	Ad_{total} (%)
30	30	176.00	20.31	196.31	61.53	6.68	33.28
60	30	209.91	18.86	228.77	37.58	7.03	27.67
90	30	298.34	18.74	317.08	50.17	10.23	40.76
30	90	171.24	50.89	222.13	56.84	5.73	18.68
60	90	187.24	50.06	237.3	41.68	7.93	21.97
90	90	208.79	47.63	256.42	47.06	10.34	28.35
30	60	173.86	49.59	223.45	59.86	8.21	24.98
90	60	218.69	27.12	245.81	39.68	7.71	27.23

Table 4 Thomas, Yoon-Nelson and Yan model parameters at 0.7 mL min^{-1} flow rate and different inlet metal ion concentrations for single biosorption of U(VI) and Ni(II) onto *C. indica* biomass

Metal ion	Q (mL min^{-1})	C_0 (mg L^{-1})	Experimental data		Yan model			Yoon-Nelson model			Thomas model		
			τ_{exp} (h)	q_{exp} (mg g^{-1})	R^2	a	q_0	R^2	τ	K_{YN}	R^2	q_0	K_{Th}
U(VI)	2.1	30	46.55	165.93	0.983	2.599	143	0.99	46.8	0.0552	0.99	221.3	0.0061
	1.4	30	113	238.64	0.978	3.78	231.6	0.994	108.1	0.0423	0.994	241.8	0.0265
	0.7	30	164.8	175.71	0.963	4.357	166.6	0.987	157.4	0.0265	0.987	281.8	0.0067
	0.7	60	69.29	194.08	0.991	3.318	176.7	0.998	68.21	0.0513	0.998	187.9	0.0131
	0.7	90	72.26	334.34	0.99	1.65	255.6	0.945	90.68	0.026	0.945	295.3	0.0056
Ni(II)	2.1	30	9.93	46.33	0.998	1.957	31.78	0.984	11.33	0.2537	0.984	39.18	0.1542
	1.4	30	8.92	52.05	0.998	1.446	29.24	0.953	18.91	0.1199	0.953	38.41	0.0826
	0.7	30	38.44	44.42	0.985	2.64	40.09	0.984	39.7	0.075	0.984	43.22	0.0487
	0.7	60	17.11	49.73	0.997	2.207	38.33	0.988	18.98	0.1594	0.988	45.02	0.0473
	0.7	90	7.25	53.47	0.998	2.948	43.62	0.996	14.68	0.2383	0.996	53.09	0.0464

bimetal solution. A general rule in heavy metal biosorption is that the more significantly changed the ions, the greater the affinity. On the other hand, the electronegativity of nickel is 1.91, which is higher than uranium electronegativity of 1.38. The cell wall of *C. indica* algae has oxygen-containing groups (negative sites) such as carboxylic, sulfonic and hydroxyl group [8]. The electron clods on oxygen atoms of those groups tend to repel the species with a higher electronegativity more forcibly. Thus, a lot of Ni(II) ions might be repelled by the negative sites on the cell wall of *C. indica*. Biosorption of U(VI) to the active sites on the biomass was, therefore, more favorable than Ni(II) ions, initially. U(VI) already adsorbed on *C. indica* might pose a physical blockage for the attachment of Ni(II) to the active sites on the surface of *C. indica*, resulting in the lower percentage removal of Ni(II) in co-biosorption with U(VI) ions.

Determination of kinetic parameters from column data modeling

The design and optimization of a fixed-bed sorption column involves the employment of mathematical models, which must be used to describe and predict the experimental breakthrough curves, in order to make the scale up of the process possible [30]. Because of this, the experimental breakthrough curves have been fitted to each one of the models mentioned previously with the aim to describe the behavior of the column for biosorption of U(VI) and Ni(II) onto *C. indica* in the single and binary component systems and to determine the corresponding kinetics parameters. The experimental breakthrough curves have been fitted to the models through non-linear regression, using the MATLAB software. The values of the parameters for single and binary mixture systems are given in Tables 4 and 5, respectively.

Single biosorption modeling

As can be seen in Table 4 for single-component systems, the Thomas model does not adequately reproduce in some cases the experimental q_0 values, allthough the regression coefficients of the model are greater than 0.945 in all cases. Also, the Thomas model cannot predict the optimum flow rate observed in the experimental data. However, the Thomas model predicts the Ni(II) adsorption better than U(VI) adsorption onto *C. indica* biomass. As indicated in Table 4, the kinetics constant of the Thomas model, K_{Th}, decrease from 0.049 to 0.046 (1 min^{-1} g^{-1}) as the inlet concentration of Ni(II) ions increases from 30 to 90 mg L^{-1}, which agrees with that obtained by other researchers. Lin et al. [20] found that for Ni(II) adsorption by IRC748 resin, the Thomas constant decreases from 0.087 to 0.024 (1 min^{-1} g^{-1}) when the inlet nickel concentration increases from 277.6 to 1109.4 mg L^{-1}. The mono metal experimental data were also fitted to Yoon-Nelson model to determine the model constants of K_{YN} and τ at different flow rates and in inlet metal concentrations. As indicated in Table 4, the regression coefficients of the Yoon-Nelson model are similar to Thomas model since the expression of the Yoon-Nelson model is mathematically analogous to the equation that represents the Thomas model. Table 4 shows that the calculated τ values from the Yoon-Nelson model are quite close to those found experimentally for U(VI) adsorption, but the model dose not reproduces the experimental τ values in some cases for Ni(II) adsorption. However, the Yoon-Nelson model can generally predict the trend of τ value changes in all conditions examined for both U(VI) and Ni(II) ions. On the other hand, the Yoon-Nelson constant, K_{YN} varies from 0.051 to 0.026 h^{-1} and from 0.075 to 0.238 h^{-1} when the inlet concentration of U(VI) and Ni(II) increases from 30 to 90 mg L^{-1}, respectively. These results agree with other

Table 5 Thomas, Yoon-Nelson and Yan model parameters at different flow rates and inlet metal ion concentrations for binary biosorption of U(VI) and Ni(II) onto *C. indica* biomass

			($C_{0,U}$, $C_{0,Ni}$) (mg L^{-1})							
			(30,30)	(60,30)	(90,30)	(30,90)	(60,90)	(90,90)	(30,60)	(90,60)
Experimental values	q_u (mg g^{-1})		176	209.91	298.34	171.24	187.42	208.79	173.86	218.69
	q_{Ni} (mg g^{-1})		20.31	18.86	18.74	50.89	50.06	47.63	49.59	27.12
	τ_U (h)		148.59	77.43	57.25	124.48	66.76	56.33	129.97	50.82
	τ_{Ni} (h)		20.39	12.01	12.99	12.34	11.34	11.61	3.61	2.23
Thomas model	U(VI)	q_0	283.3	185	230.1	146.7	175.4	198.3	292.5	201.4
		K_{Th}	0.0066	0.0107	0.0124	0.0175	0.0136	0.013	0.0054	0.0096
		R^2	0.847	0.99	0.996	0.987	0.991	0.995	0.961	0.991
	Ni(II)	q_0	27.12	12.66	16.39	41.57	33.12	34.78	10.13	6.099
		K_{Th}	0.0871	0.1454	0.2155	0.0548	0.065	0.0612	0.186	0.2979
		R^2	0.996	0.997	0.999	0.999	0.998	0.998	0.94	0.95
Yoon-Nelson model	U(VI)	τ	238.9	79.56	61.6	127.8	71.61	60.59	231.8	51.65
		K_{YN}	0.0112	0.0355	0.066	0.0285	0.0473	0.0604	0.0097	0.0533
		R^2	0.847	0.99	0.996	0.987	0.991	0.995	0.961	0.991
	Ni(II)	τ	21.25	11.33	13.97	12.29	9.628	10.23	3.857	2.451
		K_{YN}	0.1575	0.2307	0.3388	0.2635	0.3177	0.2955	0.6925	1.053
		R^2	0.996	0.997	0.999	0.999	0.998	0.998	0.94	0.95
Yan model	U(VI)	q_0	132.5	168.3	204.4	141.9	161.7	173.3	146.4	149.2
		a	4.88	2.241	3.189	3.243	2.99	2.932	2.325	1.856
		R^2	0.987	0.99	0.999	0.997	0.999	0.999	0.9398	0.999
	Ni(II)	q_0	25.01	9.08	15.08	29.07	23.33	24.08	5.18	10.44
		a	3.016	2.408	3.464	2.597	3.035	3.118	0.804	1.21
		R^2	0.991	0.995	0.999	0.999	0.999	0.997	0.965	0.955

researchers studying different solute-sorbent systems [26, 32, 42, 43]. For example, Calero et al. [35], studying Cr(III) sorption by olive stone, indicated that the K_{YN} constant varies between 0.381 and 250 h^{-1} when the concentration increases from 10 to 100 mg L^{-1}. The Yan model is also used to describe column biosorption data. The model parameters (a and q_0) are given in Table 4. As can be seen in Table 4, the regression coefficients of the Yan model are greater than 0.963 in all cases. Also, the q_0 values of the model are very close to those found experimentally for both U(VI) and Ni(II) ions. If all the models used are compared, it can be concluded that the Yan model is the one which best reproduce the breakthrough curves for all conditions examined in this study for both U(VI) and Ni(II) ions. The breakthrough curves predicted by the Yan model for mono-metal systems were shown in Figs. 1 and 2. As can be seen from these figures, the predicted breakthrough curves showed reasonably good agreement with the experimental curves. These results, in terms of both the value of the parameters and the reproduction of the experimental data through the Yan model are similar to those found by other researchers working on different sorbate-sorbent systems [16, 35, 40, 43, 44].

Binary biosorption modeling

In order to model the effect of coexistence ions on the adsorption of *C. indica* biomass, the experimental data for binary-component metal ions (U(VI)–Ni(II)) were fitted to the Thomas, Yoon-Nelson and Yan models. As can be seen in Table 5, the regression coefficients of the Thomas, Yoon-Nelson and Yan models are greater than 0.847, 0.847 and 0.939, respectively for U(VI) ions adsorption and 0.940, 0.940 and 0.955, respectively for Ni(II) ions adsorption, in all conditions examined in this study. Also, it is observed that the Thomas model rate constant (K_{Th}) for both metal ions increased with the increasing inlet metal ion concentration. In addition, the Yoon-Nelson model rate constant (K_{YN}) follows the same trend as that of the Thomas model rate constant. The same results were observed by Aksu et al. [32] for studying the binary biosorption of phenol and Cr(VI) onto immobilized activated sludge in a packed bed column. They noticed that this behavior is because the driving force of mass transfer in the liquid film is increased. The data in Table 5 indicated that there are either negligible or significant differences between the experimental and predicted values of q_i and τ_i for binary

mixture. These deviations are not surprising, considering that both kinetic parameters of each component depended on the assumed breakthrough curve function which was derived for a single-component adsorption and used for binary mixture. Moreover, the Thomas and Yoon-Nelson equations predicted a non-zero effluent concentration at $t = 0$ which contradicted real conditions. The model parameters (a_i, $q_{0,i}$) of the Yan equation have been given in Table 5 for both metal ions. Comparing the maximum uptake capacities ($q_{0,\,cal}$) of U(VI) and Ni(II) on *C.indica* biomass predicted by the Yan model with the experimental uptake values (q_{exp}), it is observed that the predicted values agree well with the experimental data for both metal ions. These results coincide with Yan et al. [36] observations. They concluded that the use of the Yan model minimizes the error resulting from the use of the Thomas model, especially at lower or higher time periods of the breakthrough curve. The dynamic behavior of the column for each component in binary mixtures predicted with the Yan model was shown in Figs. 3, 4, and 5. Among these models, the Yoon-Nelson with higher regression coefficients values ranging from 0.939 to 0.999 could describe the breakthrough data better than the Thomas and Yoon-Nelson models for both U(VI) and Ni(II) ions in the binary mixture.

Conclusions

From experimental results of the single and binary biosorption of U(VI) and Ni(II) ions onto Ca-pretreated *C. indica* biomass in a fixed-bed column, the following conclusions can be drawn:

1. The breakthrough and exhaustion time decrease with the increase of the flow rate for both metal ions in a single aqueous solution. The same effect is shown when the inlet metal concentration increases. Also, the breakthrough curves become steeper and shift to the left with increasing flow rate or inlet metal concentration for both metal ions. In addition, it is observed that the controlled-rate step shifts from external to internal mass transfer limitations, as the flow rate increase and an optimum flow rate equal to 1.4 mL min^{-1} is obtained for both metal ions. Moreover, the effect of flow rate on the single component biosorption shows that it is possible to choose an appropriate flow rate in order to separate U(VI) ions from Ni(II) ions by a *C. indica* fixed-bed column.
2. The data obtained in the single systems indicate that the adsorption capacity of *C. indica* for both metal ions increases with the increasing inlet concentration of each component and also, the uptake capacity of *C. indica* for U(VI) ions is higher than that of Ni(II) ions. The same behavior is observed in the binary systems. From the single and binary biosorption data, it was concluded that the algae *C. indica* presents greater adsorption affinity for U(VI) compared with Ni(II).
3. The data obtained in the binary systems indicate that the presence of the second component decreased the capacity of the first component and by increasing the inlet concentration of the second component in the binary mixture, the breakthrough curve of the first component becomes steeper and shifts to the left. So, it is concluded that the combined action of U(VI) and Ni(II) ions is antagonistic. Also, it was observed that the presence of U(VI) ions greatly affected the uptake of Ni(II) ions rather than that of the presence of Ni(II) ions in U(VI) containing solution.
4. Thomas, Yoon-Nelson and Yan models were applied to the experimental data obtained from the single and binary biosorption of U(VI) and Ni(II) ions onto *C. indica.* Among these models, the best fit of the U(VI) and Ni(II) breakthrough curves, obtained under different experimental conditions tested, was achieved with the Yan model in both single and binary systems.
5. This study indicated that the Ca-pretreated *C. indica* biomass could be used as an efficient biosorption bed in the fixed-bed columns for the removal of U(VI) and Ni(II) ions bearing wastewater streams because, *C. indica* is an inexpensive, easily available biomaterial with high adsorption capacity for both metal ions.

References

1. Apiratikul R, Pavasant P (2008) Biores Tech 99:2766–2777
2. Bozkurt SS, Molu ZB, Cavas L, Merdivan M (2011) J Radioanal Nucl Chem 288:867–874
3. Han R, Zhang J, Zou W, Xiao H, Shi J, Liu H (2006) J Hazard Mater B133:262–268
4. Donat R, Esen K, Cetisli H, Aytas S (2009) J Radioanal Nucl Chem 279:253–261
5. Hawari AH, Mulligan CN (2006) Process Biochem 41:187–198
6. Hafez MB, Ibrahim MK, Abdel-Razek AS, Abu-Shady MR (2002) J Radioanal Nucl Chem 252:179–185
7. Vilar VJP, Loureiro JM, Botelho CMS, Boaventura RAR (2008) J Hazard Mater 154:1173–1182
8. Davis TA, Volesky B, Mucci A (2003) Water Res 37:4311–4330
9. Naddafi K, Nabizadeh R, Saeeidi R, Mahvi AH, Vaezi F, Yaghmaeian K, Ghasri A, Nazmaraa S (2007) J Hazard Mater 147: 785–791
10. Akhtar K, Khalid AM, Akhtar MW, Ghauri MA (2009) Biores Tech 100:4551–4558
11. Charrier MJ, Guibal E, Roussy J, Surjous R, Cloirec PL (1996) Water Sci Tech 34:169–177
12. Tsezos M, McCready RGL, Bell JP (1989) Biotech Bioeng 34:10–17
13. Tsuruta T (2007) Am J Environ Sci 3:60–66

14. Zou W, Zhao L, Han R (2009) J Chem Eng 17:585–593
15. Akhtar N, Iqbal J, Iqbal M (2004) J Hazard Mater 108(1–2): 85–94
16. Borba CE, Guirardello R, Silva EA, Veit MT (2006) Biochem Eng J 30:184–191
17. Doan HD, Lohi A, Dang VBH, Dang-Vu T (2008) Process Saf Environ Prot 86:259–267
18. Gupta BS, Curran M, Hasan S, Ghosh TK (2009) J Environ Manage 90:954–960
19. Li C, Champagne P (2009) J Hazard Mater 171:872–878
20. Lin LC, Li JK, Juang RS (2008) Desalination 225:249–259
21. Vijayaraghavan K, Jegan J, Palanivelu K, Velana M (2004) J Hazard Mater B113:223–230
22. Vijayaraghavan K, Jegan J, Palanivelu K, Velana M (2005) Chemosphere 60:419–426
23. Khani MH, Keshtkar AR, Ghannadi M, Pahlavanzadeh H (2008) J Hazard Mater 150:612–618
24. Pahlavanzadeh H, Keshtkar AR, Safdari J, Abadia Z (2010) J Hazard Mater 175(1–3):304–310
25. Montazer-Rahmati MM, Rabbania P, Abdolalia A, Keshtkar AR (2011) J Hazard Mater 185(1):401–407
26. Aksu Z, Gönen F (2003) Process Biochem 39:599–613
27. Chu KH (2004) J Chem Eng 97:233
28. Kratochvil D, Volesky B (2000) Water Res 34:3186
29. Zulfadhly Z, Mashitah MD (2001) Environ Pollut 112:463
30. Lodeiro P, Herrero R, Vicente MESd (2006) J Hazard Mater B137:244–253
31. Volesky B, Weber J, Park JM (2003) Water Res 37:297–306
32. Aksu Z, Gonen F (2006) Sep Purif Tech 49:205–216
33. Thomas HC (1944) J Am Chem Soc 66:1664–1666
34. Yoon YH, Nelson JH (1984) Am Ind Hyg Assoc J 45:509
35. Calero M, Hernainz F, Blazquez G, Tenorio G, Martin-Lara MA (2009) J Hazard Mater 171:886–893
36. Yan G, Viraraghavan T, Chen M (2001) Adsorpt Sci Tech 19:25–43
37. Vieira MGA, Oisiovici RM, Gimenes ML, Silva MGC (2008) Biores Tech 99:3094–3099
38. Han R, Zou W, Li H, Li Y, Shi J (2006) J Hazard Mater B137:934–942
39. Preetha B, Viruthagiri T (2007) Sep Purif Tech 57:126–133
40. Vijayaraghavan K, Prabu D (2006) J Hazard Mater B137: 558–564
41. Sag Y, Atacoglu I, Kutsal T (2000) Hydrometallurgy 55:165–179
42. Ozturk N, Kavak D (2004) Adsorption 10:245–257
43. Senthilkumar R, Viraraghavan K, Thilakavathi M, Iyer PVR, Velan M (2006) J Hazard Mater 136:791–799
44. Vaughan RL, Reed BE, Jensen JE, Gang DD, Smith EH, Deng B (2002) Water Environ Res 74:231–342